Random Body Movement Mitigation for FMCW-Radar-Based Vital-Sign Monitoring

José-María Muñoz-Ferreras[1], Zhengyu Peng[2], Roberto Gómez-García[1], and Changzhi Li[2]

[1]Dept. Signal Theory & Commun., University of Alcalá, Alcalá de Henares, 28871, Madrid, SPAIN
[2]Dept. Electrical & Computer Engineer., Texas Tech University, Lubbock, TX 79409, USA

***Abstract*— In noncontact vital-sign-monitoring applications, the cancelation of the random body movement (RBM) becomes critical for a proper tracking. When using Doppler radars, this RBM suppression has been typically carried out through phase measurements obtained from two opposite sides of the human body. In this work, the employment of two frequency-modulated continuous-wave (FMCW) radars to deal with the RBM phenomenon is proposed. An advanced range-bin alignment technique is utilized to derive the range histories from the two transceivers and proceed with the RBM mitigation. Moreover, since this approach is only based on the signal amplitudes, the FMCW radar sensors do not need to be coherent. Simulated results are also reported to corroborate the effectiveness of the devised RBM suppression technique.**

***Index Terms*— Biomedical radars, Doppler radars, frequency-modulated continuous-wave (FMCW) radars, random body movement (RBM), vital-sign monitoring.**

I. Introduction

Measurements of vital signs (e.g., respiration and heartbeats) through noncontact radars are usually accurate if the patient remains static during the illumination time [1]. This hinders the application of radars in some interesting biomedical scenarios, such as the monitoring of vital signs when the person is sleeping (e.g., for apnea detection and assessment) [2]. Note that, in this case, the subject may be moving during some periods. Hence, it is normally decided that no vital-sign information from the radar sensors can be retrieved during these random-body-moving intervals [2].

This unwanted motion—hereafter referred to as random body movement (RBM)—can be much larger than that associated with the weak and slow vital signs to be measured. Thus, it comes clear that the successful tracking of the aforementioned vital signs can become a very challenging task. However, an innovative approach to mitigate RBM was proposed in [3]. It demonstrated that by illuminating the subject from two opposite sides of the body (e.g., from the front and the back) and combining the measurements, it is possible to reduce these undesired motions [3].

The approach of [3] makes use of two Doppler prototypes. These continuous-wave (CW) radars exploit phase measurements to retrieve the range history from targets, but they do not possess range resolution (i.e., they do not transmit an instantaneous bandwidth). The application of frequency-modulated continuous-wave (FMCW) radars to monitor vital signs was proposed in [4]. Deramping-based FMCW radars do have range resolution, leading to advantages in terms of range-isolation capabilities, ease of implementation, and ability to recover original movement patterns [4].

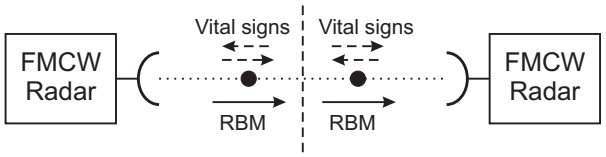

Fig. 1. Schematic representation of the vital-sign-monitoring scenario: two FMCW radars illuminate two opposite sides of the monitored patient.

In this work, the employment of two FMCW radars to illuminate two opposite sides of the patient is suggested to mitigate the RBM phenomenon. By combining the range histories obtained by each radar sensor, the vital signs can be accurately tracked. The extraction of these range evolutions is achieved by means of a range-bin alignment method adopted from the inverse synthetic aperture radar (ISAR) research field [5]. In particular, a subinteger envelope correlation approach is utilized [6]. Furthermore, the technique works for incoherent FMCW radars, which noticeably simplifies the design and construction of the required prototypes. Simulated results are also expounded to verify the suitability of the conceived FMCW-radar-based method for RBM cancelation.

II. Principle of Operation

A schematic representation of the acquisition scenario is shown in Fig. 1. The two depicted scatterers represent the front and the back of the person to be monitored. It is assumed here that each FMCW radar only receives echoes from its corresponding nearest scatterer.

As depicted in Fig. 1, the RBM (continuous arrows) has the same direction sense for both scatterers, whereas the motion associated with the vital signs (dashed arrows) has opposite direction senses. This can be easily visualized by noting that the lungs and heart expand and contract

periodically. As a consequence, the ranges to the front and back scatterers can be respectively expressed as

$$R_f(\tau) = R_{0f} + R_{rbm}(\tau) + R_r(\tau) + R_h(\tau) \quad (1)$$

$$R_b(\tau) = R_{0b} - R_{rbm}(\tau) + R_r(\tau) + R_h(\tau) \quad (2)$$

where τ is the slow time, R_{0f} and R_{0b} are the initial ranges from the FMCW radars to the corresponding scatterers, $R_{rbm}(\tau)$ is the displacement for the RBM, $R_r(\tau)$ is the range variation due to the respiration, and $R_h(\tau)$ is the displacement associated with the heartbeat vital sign.

Although any waveform may be considered, the vital signs are here assumed to follow a sinusoidal pattern. That is, the displacements $R_r(\tau)$ and $R_h(\tau)$ are formulated as

$$R_r(\tau) = A_r \sin(2\pi f_r \tau) \quad (3)$$

$$R_h(\tau) = A_h \sin(2\pi f_h \tau) \quad (4)$$

where A_r and A_h are the amplitudes of the respiration and heartbeat vital signs respectively, and f_r and f_h are their respective frequencies.

Once the ranges $R_f(\tau)$ and $R_b(\tau)$ for the two FMCW radars have been obtained (see Section III), a simple way to estimate the displacement history for the compound vital sign ($R_r(\tau) + R_h(\tau)$) consists of adding the two range estimates $R_f(\tau)$ and $R_b(\tau)$ and dividing the result by two, as it can be directly inferred from (1) and (2). Note that the constant terms R_{0f} and R_{0b} are unimportant.

A Fourier transform applied to the recovered compound signal ($R_r(\tau) + R_h(\tau)$) leads to two peaks corresponding to the frequencies of the respiration and heartbeat vital signs, which can be exploited for detection purposes.

III. Amplitude-Based Range Tracking for Incoherent FMCW Radars

The range resolution of a radar refers to its ability to discriminate two targets closely spaced in range. The range resolution Δ_R is given by [4]

$$\Delta_R = \frac{c}{2B} \quad (5)$$

where c is the speed of light and B is the instantaneous transmitted bandwidth.

A deramping-based FMCW radar obtains a range profile for each transmitted period after applying a Fourier transform to the so-called baseband "beat signal", which is the result of mixing a replica of the transmitted signal with the returned echoes [4].

For both of the required FMCW radars, a corresponding range-slow-time matrix—i.e., the range profiles—can be constructed [4]. Even if the radar is incoherent—i.e., it cannot obtain phase/Doppler information—, the construction of this range-profile matrix is feasible.

If the RBM is large enough, it is possible that the target signature migrates through range cells. From the ISAR literature, one can find method to align the echoes (see [5] and cites therein). Among these range-bin alignment methods, the subinteger envelope-correlation approach is here chosen [6] due to its capability of aligning the echoes with sub-cell accuracy [6]. Furthermore, it is robust against the target-scintillation phenomenon as an added benefit [6].

From the alignment process, the range histories $R_f(\tau)$ and $R_b(\tau)$ associated with the FMCW radar sensors can be estimated. These tracks are then used for the RBM mitigation and vital-sign recovery, as Section II describes.

TABLE I
Parameters of the FMCW Radars

Center frequency (f_c)	10 GHz
Transmitted bandwidth (B)	1.5 GHz
Waveform period (T)	20 ms
Acquisition time	10 s

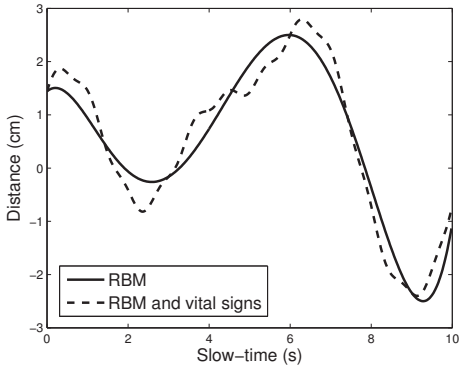

Fig. 2. Range history for the RBM (continuous line) and for the RBM plus vital signs (dashed lines) for the simulated example.

IV. Simulated Results

In this section, the previous ideas for RBM mitigation are verified for a simulated example. To this aim, let it consider the scenario in Fig. 1. The parameters of the two FMCW radars are detailed in Table I. Note that a periodic sawtooth waveform has been assumed for them [4].

According to (5), the range resolution for the radars is $\Delta_R = 10$ cm. The simulated RBM has a peak-to-peak amplitude of 5 cm, as shown in Fig. 2 (continuous line). The displacement corresponding to the RBM and the vital signs (equation (1)) is also plotted in Fig. 2 (dashed line). The rest of parameters describing the motion of the scatterers are listed in Table II. As observed, the RBM displacement is much larger than the one for the vital signs. Indeed, as shown later, a Fourier transform applied to a single range history (e.g., $R_f(\tau)$) does not enable detection of the respiration and heartbeat rates.

The range-profile matrix for the front radar is shown in Fig. 3. Despite the fact that the range resolution ($\Delta_R = 10$ cm) is larger than the peak-to-peak amplitude of the

TABLE II

PARAMETERS FOR THE SCENARIO IN FIG. 1

Initial range to the front scatterer (R_{0f})	2 m
Initial range to the back scatterer (R_{0b})	2 m
Amplitude of respiration (A_r)	5 mm
Amplitude of heartbeats (A_h)	1 mm
Frequency of respiration (f_r)	20 cycles/min
Frequency of heartbeats (f_h)	70 beats/min

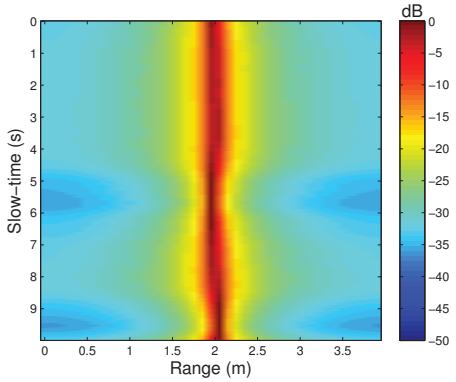

Fig. 3. Range-profile matrix for the front FMCW radar.

compound RBM plus vital signs (see Fig. 2), a non-perfect alignment of the scatterer echo can be visualized.

After applying the range-bin alignment method in [6], the echoes corresponding to the front scatterer are properly aligned. This is shown in Fig. 4. Note that the sub-cell alignment capability of the extended envelope-correlation method in [6] provides a good output. Similar results are derived for the back scatterer.

Given the estimates of $R_f(\tau)$ and $R_b(\tau)$ after the alignment stage, their half-sum provides the reconstruction of the compound vital signs (see Fig. 5 (top)) with the RBM properly mitigated. Fig. 5 (bottom) shows the result of applying a Fourier transform to this estimate of $R_r(\tau)+R_h(\tau)$. Two peaks corresponding to the respiration and heartbeats are clearly identifiable. The spectrum for the range estimate $R_f(\tau)$ is also shown in Fig. 5 (bottom), where the vital signs cannot be detected. This reveals the importance of properly suppressing the unwanted RBM in the addressed vital-sign-remote-sensing scenario.

V. CONCLUSION

A method for RBM mitigation to monitor vital signs with incoherent FMCW radars has been reported. Two FMCW radars illuminating two opposite sides of the body are used. Also, a sub-cell range-bin alignment technique to extract the associated range histories has been employed. The approach has been verified using simulated data.

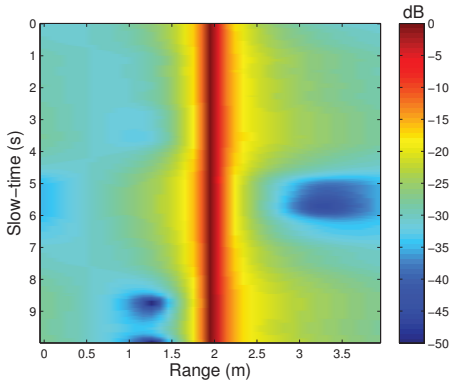

Fig. 4. Range-profile matrix for the front FMCW radar after applying the range-bin alignment method in [6].

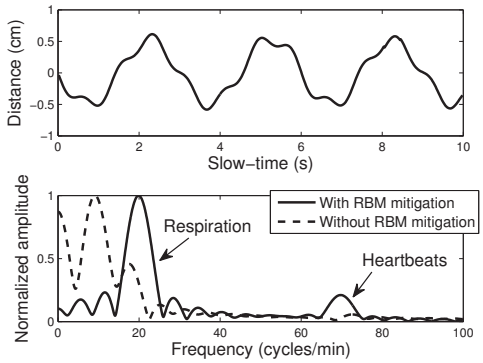

Fig. 5. Time-domain history (top) and spectrum (bottom, continuous line) of the compound vital signs after the RBM cancelation method. The spectrum without RBM cancelation (dashed line) is also shown in the bottom subfigure.

ACKNOWLEDGMENT

This work was partially supported by the Spanish Government under Project TEC2014-54289-R.

REFERENCES

[1] C. Li, V. M. Lubecke, O. Boric-Lubecke, and J. Lin, "A review on recent advances in Doppler radar sensors for noncontact healthcare monitoring," *IEEE Trans. Microw. Theory Techn.*, vol. 61, no. 5, pp. 2046–2060, May 2013.

[2] M. Baboli, A. Singh, B. Soll, O. Boric-Lubecke, and V. Lubecke, "Good night: sleep monitoring using a physiological radar monitoring system integrated with a polysomnography system," *IEEE Microw. Mag.*, vol. 16, no. 6, pp. 34–41, Jul. 2015.

[3] C. Li and J. Lin, "Random body movement cancellation in Doppler radar vital sign detection," *IEEE Trans. Microw. Theory Techn.*, vol. 56, no. 12, pp. 3143–3152, Dec. 2008.

[4] G. Wang, J. M. Muñoz-Ferreras, C. Gu, C. Li, and R. Gómez-García, "Application of linear-frequency-modulated continuous-wave (LFMCW) radars for tracking of vital signs," *IEEE Trans. Microw. Theory Techn.*, vol. 62, no. 6, pp. 1387–1399, Jun. 2014.

[5] X. Li, G. Liu, and J. Ni, "Autofocusing of ISAR images based on entropy minimization," *IEEE Trans. Aerosp. Electron. Syst.*, vol. 35, no. 4, pp. 1240–1252, Oct. 1999.

[6] J. M. Muñoz-Ferreras and F. Pérez-Martínez, "Subinteger range-bin alignment method for ISAR imaging of noncooperative targets," *EURASIP J. Adv. Signal Process.*, vol. 2010, no. 1, pp. 1–16, Jan. 2010.